PRAMANA — journal of physics

Vol. 85, No. 6
Month 2015
pp. 1207–1219

Imperative function of electron beams in low-energy plasma focus device

M Z KHAN[1,2,*], L K LIM[1], S L YAP[1] and C S WONG[1]

[1]Plasma Technology Research Centre, Department of Physics, Faculty of Science, University Malaya, 50603 Kuala Lumpur, Malaysia
[2]Department of Physics, Federal Urdu University of Arts, Science and Technology, 45320 Islamabad, Pakistan
*Corresponding author. E-mail: mzubairkhan_um76@yahoo.com

MS received 1 October 2013; revised 7 June 2014; accepted 27 September 2014
DOI: 10.1007/s12043-015-0951-6; ***e*Publication:** 12 April 2015

Abstract. A 2.2 kJ plasma focus device was analysed as an electron beam and an X-ray source that operates with argon gas refilled at a specific pressure. Time-resolved X-ray signals were observed using an array of PIN diode detectors, and the electron beam energy was detected using a scintillator-assisted photomultiplier tube. The resultant X-rays were investigated by plasma focus discharge for pressures ranging from 1.5 mbar to 2.0 mbar. This range corresponded to the significant values of X-ray yields and electron beam energies from the argon plasma. The electron temperature of argon plasma at an optimum pressure range was achieved by an indirect method using five-channel BPX65 PIN diodes of aluminum foils with different thicknesses. X-ray yield, electron beam energy, and electron temperature of argon plasma were achieved at 1.5–2.0 mbar because of the strong bombardment of the energetic electron beam.

Keywords. Dense plasma focus; X-ray yield; electron beam energy; photomultiplier tube; X-ray spectrometer.

PACS Nos 52.58.Lq; 52.59.Hq; 52.59.Px

1. Introduction

Mather-type dense plasma has been used to explore radiation emissions, electrons, and ion beams [1]. Plasma focus devices are widely applied sources of energetic electron beam emission. Plasma focus device has been utilized in X-ray and electron beam lithography [2–4], radiography of biological specimens [5], metal coating by ion sputtering [6], micromachining [7], X-ray backlighting [8,9], contact microscopy [10], and generation of soft X-ray (SXR) spectral lines of highly charged heavy metal ions [11] because of its simplicity, uncomplicated maintenance, and compactness. In addition, plasma focus is a potential device for generating X-rays with enhanced efficiency because of its high X-ray yield [12].

Short-lived, high-density, and high-temperature plasma is created at the final phase of plasma focus discharge [13], which is a primary source of intense X-ray emission. The plasma temperature is higher than 1 keV, and the emitted radiation is mainly due to bremsstrahlung emission of hydrogen and its isotopes. The electron temperature of plasma focus can be indirectly determined by analysing the radiation spectrum [14]. Bernstein [15] performed time-resolved measurement of emitted spectra of deuterium plasma focus discharge to determine the correlation of X-ray and neutron emissions. He found that periods of X-rays with various energies corresponded to those of neutron emissions. Two periods of neutron emissions are typically observed in plasma focus discharge, and these periods are associated with the thermal and acceleration mechanisms [16]. Results of SXR measurements from a low-energy plasma focus of 345 J at 7 mbar hydrogen in a previous study revealed several periods of weak X-ray emissions. SXR pulses were generally correlated in time with peak voltage and current dip, which indicated the pinch and post-pinch phases [17]. Al-Hawat *et al* [18] investigated the effects of copper impurities on the electron temperature of low-energy Mather-type plasma (energy, 2.8 kJ; potential, 15 kV) in AECS PF-2. They estimated the electron temperature with argon gas using X-ray ratio method with Al foils of different thicknesses. Five-channel BPX65 PIN diodes were employed to record the X-ray signals. The temperature of argon plasma was calculated by comparing the ratio between the experimentally obtained and theoretically calculated values. The electron temperatures ranging from 1.5 to 2.5 keV for argon plasma was obtained, in which the X-ray emission was Cu-K_α radiation for most of the discharges. Hussain *et al* [19] have generated an X-ray radiogram of a fish in a high-intensity X-ray source for contrast biological radiography. Zakaullah *et al* [20] investigated the X-ray emission from a low-energy plasma focus device with argon gas and found that the radiation was due to the interaction between the energetic electron beam and the anode. The calculated X-ray yield was 30 mJ with 0.0015% efficiency in 4π sr. at 1.5 mbar, and the total yield was 0.7 J in 4π sr. with a device efficiency of $\sim$0.028%. Furthermore, they found that the total X-ray yield was due to the strong interactions between the energetic electron beam and the anode.

Different methods have been used to analyse the emissions of energetic electron beam from the dense plasma focus. These methods include analyses of hard X-ray spectrum [21,22], Rogowski coil (RC) [23], magnetic energy analyser [24,25], and Faraday cup [26–28].

In this study, we discuss the important functions of the energetic electron beam in low-energy plasma focus using an array of PIN diode detectors, XR100CR X-ray spectrometer, and a scintillator-assisted photomultiplier tube. Electron temperature, X-ray yield, and energy of the energetic electron beam were determined in argon plasma at pressures ranging from 1.5 to 2.0 mbar.

2. Experimental details

The experiments were performed on the Mather-type plasma focus device. The device was energized by a 30 μF Maxwell capacitor, which was charged up to 12 kV. A small piece of lead rod with 1.5 cm diameter and 0.35 cm width was used as the target material.

The total external inductance of the system was found to be 165 nH. The schematic of the low-energy plasma focus device is shown in figure 1.

The discharge tube consisted of a copper electrode, i.e., the inner electrode was a hollow cylinder as the anode with 1.9 cm diameter and 18 cm effective length. The hollow anode was used in the experiment to observe the energetic electron beam in the plasma focus device. The outer electrode consisted of a group of six copper rods that formed a shape of a squirrel cage with an inner diameter of 3.2 cm (figure 2).

The length of each cathode rod was 27 cm, which was 9 cm more than that of the anode rod. A pyrex glass was used as an insulator to separate the hollow anode and the cathode. The rotary pump in the vacuum system reduced the chamber pressure to $<10^{-2}$ mbar, which was sufficient for this experiment. The chamber was refreshed after every shot to reduce contamination of gas with impurities from the output radiation. The argon gas was refilled to the desired pressure.

All the 110 cm long coaxial cables were protected with an aluminum (Al) foil to reduce the effects of electromagnetic noise on data signals. Two DPO4043 digital storage oscilloscopes were used to record the signals from the energetic electron beam passing through the Faraday cup and those from the Rogowski coil (RC), high-voltage (HV) probe, and five-channel PIN diode. The oscilloscope was simultaneously triggered for all electrical signals. Five PIN diode detectors were normalized against each other by covering each with identical aluminized Mylar foils (thickness=23 μm). The PIN diode response ranged between 1 and 30 keV. Combinations of filters were used to view different spectral windows.

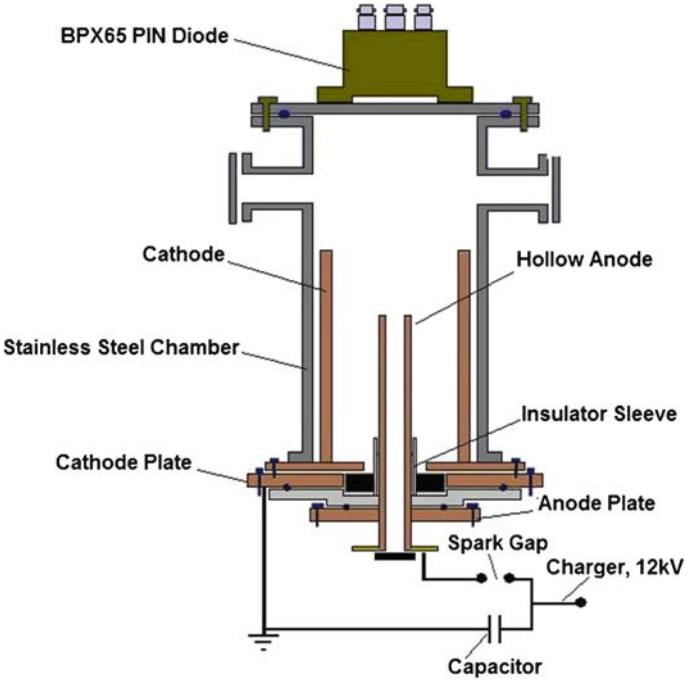

Figure 1. Schematic of the plasma focus device.

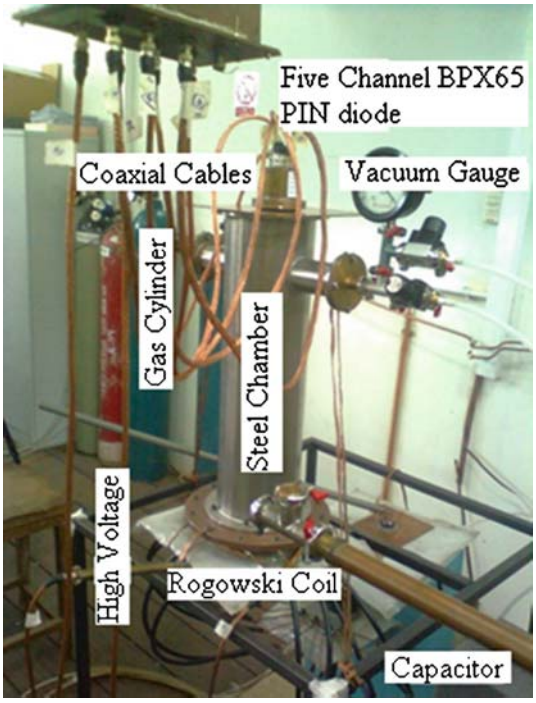

Figure 2. Picture of the plasma focus system.

The R928 photomultiplier tube (PMT) coupled with a cylindrical plastic scintillator was positioned at 4 ± 0.5 cm from the target, which was adjusted to 37 cm from the focus and within the hollow anode (figure 3).

An XR100CR X-ray spectrometer was used to record the X-ray line spectra at the top- and side-on of the system by the collision of the energetic electron beam with the lead target (figure 4).

This spectrometer is sensitive up to 45 keV and can be used for the analysis and determination of the X-ray energy distribution.

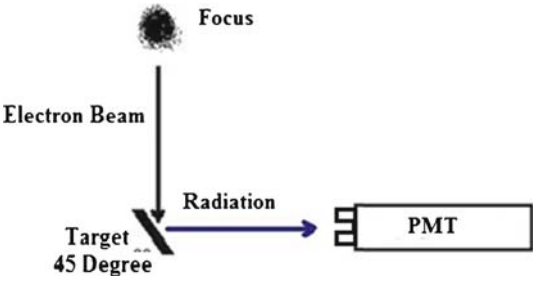

Figure 3. The R928 photomultiplier tube (PMT) coupled with a scintillator.

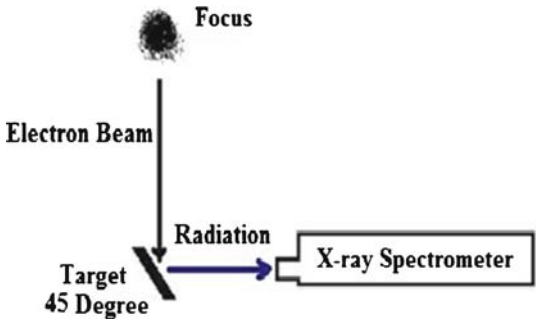

Figure 4. X-ray spectrometer position at the side-on of the system with the target at an angle of 45°.

3. Results and discussion

X-ray emissions from plasma focus operated under argon gas were investigated by time-resolved five-channel BPX65 PIN diode. The design parameters of the device are summarized in table 1.

RC and HV probes were used to measure the total discharge current and voltage signals, respectively. Typical signals of RC and HV probes are shown in figure 5.

An array of five filtered PIN diodes was placed 43.50 cm from the hollow anode head to measure radiation emission from the focussed plasma and to detect X-rays. The glass window of the PIN diode was detached to detect X-ray emissions. PIN diode responses ranged between 0.5 and 30 keV [29]. The diode window was then covered with Al foils of specific thickness (table 2).

The circuit of the BPX65 diode was designed with reverse bias at −45 V (figure 6).

The transmission curves of the BPX65 diode were attached with the associated absorption filters (figure 7).

The X-ray yield in 4π-geometry and the system efficiency of X-ray emission were calculated using five-channel PIN diodes covered with Al foil. This yield is given as [30,31]

$$Y = \frac{Q_{\exp}(4\pi)}{\mathrm{d}\Omega S(E)T(E)},$$

where $Q_{\exp} = \int \frac{V\mathrm{d}t}{R}$ (C), ($\int V\mathrm{d}t$ is the area under the curve with PIN diode's filter and $R = 50\ \Omega$ (in experiments)), $S(E)$ is the average sensitivity of the detector, $T(E)$ is the average transmission of the filter, $\mathrm{d}\Omega = \mathrm{d}A/r_0^2$ (sr.) is the solid angle subtended by

Table 1. Design parameters of the plasma focus system.

Component	Length (cm)	Diameter (cm)	Material
Hollow anode	18.00	1.90/1.60 (OD/ID)	Copper
Cathode rod	27.20	0.95	Copper
Insulator sleeve	5.00	2.00	Pyrex
Faraday cup plate	0.1	0.75	Copper

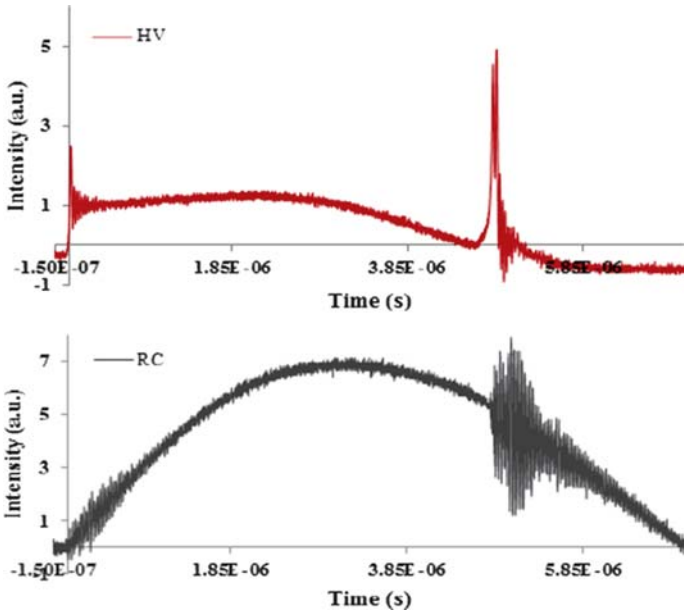

Figure 5. Typical Rogowski coil signal with high-voltage probe.

the detector at the centre of the anode where $dA = \pi r^2$. Here, r is the radius of the exposed area of each detector while r_0 is the distance from the detector to the hollow anode.

Variations in X-ray emission as functions of the argon gas pressure efficiently generated radiation in plasma focus devices. In our experiment, different pairs of Al foils or Ross filters (20 and 100 μm; 30 and 100 μm; and 40 and 100 μm) were used to determine the X-ray yield. Variations in the average signal intensities at distinct argon gas pressures are shown in figure 8.

The maximum average signal intensity was observed for 20, 30, and 40 μm Al foils at 1.7 mbar argon gas pressure. In our plasma focus device, the maximum intensity of radiation was observed for argon pressures ranging from 1.5 to 2.0 mbar due to the strong effect of electron beams on the target within the hollow anode.

Variations in the total X-ray yield and efficiency vs. argon gas pressures at a constant applied voltage of 12 kV are shown in figure 9.

Table 2. Five PIN diodes covered with Al foils+aluminized Mylar (μm).

PIN diode	Filter	Thickness (μm)
1	Aluminized Mylar	23
2	Al+aluminized Mylar	23+20
3	Al+aluminized Mylar	23+30
4	Al+aluminized Mylar	23+40
5	Al+aluminized Mylar	23+100

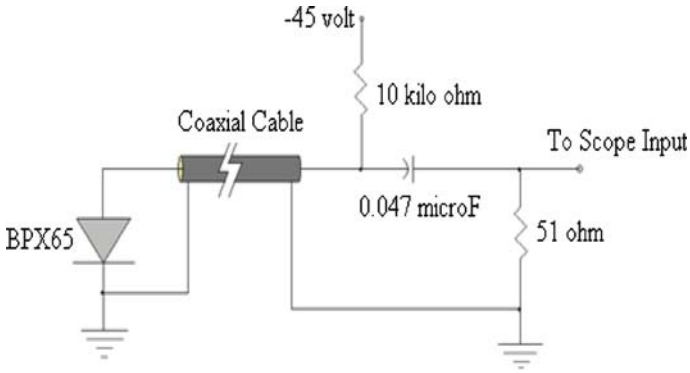

Figure 6. The basic circuit of the BPX65 PIN diode.

The maximum X-ray yield was obtained at 1.7 mbar with constant voltage of 12 kV using pairs of Al foils with varying thickness: 20 and 100 μm; 30 and 100 μm; and 40 and 100 μm. The corresponding maximum total X-ray yields were found to be 77, 47, and 42 mJ with corresponding efficiencies of 0.0035, 0.0021, and 0.0018% in 4π-geometry. The Al foils were fixed exactly on top of the hollow anode tip at a distance of 43.50 cm. The energetic electron beam interacted with the lead target placed at a depth of 27 cm within the hollow anode. Radiations were emitted from the focus and penetrated through the Al foils after collision with the target in the hollow anode. The total radiation yield obtained by strong interactions of the electron beam with the hollow anode was observed for pressures ranging from 1.5 to 2.0 mbar.

The X-ray signal ratio $R = I/I_0$, where I is the absorbed intensity and I_0 is the intensity, was calculated against different Al foil thicknesses for electron temperatures

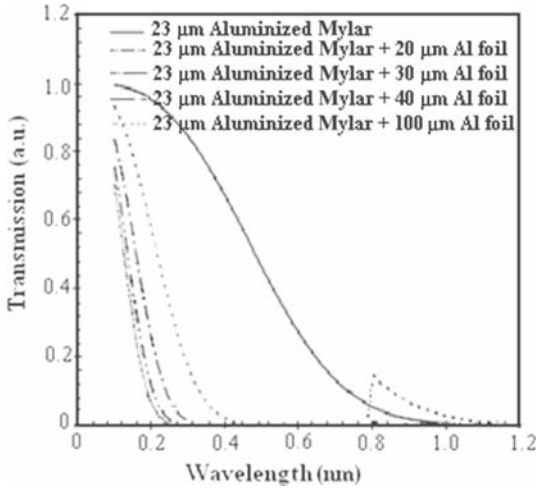

Figure 7. Transmission curves of 23 μm aluminized Mylar, 23 μm aluminized Mylar + (20, 30, 40, and 100 μm) Al foils.

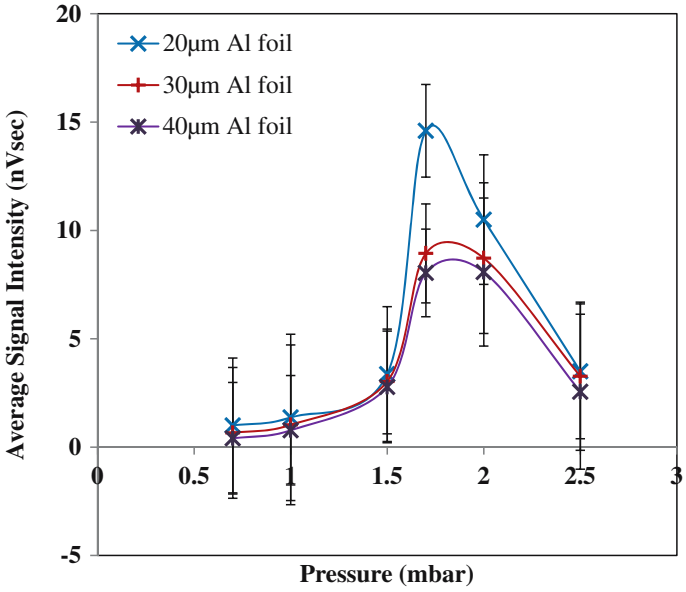

Figure 8. Variations in average signal intensities recorded at 20, 30, and 40 μm Al foils vs. argon gas pressure.

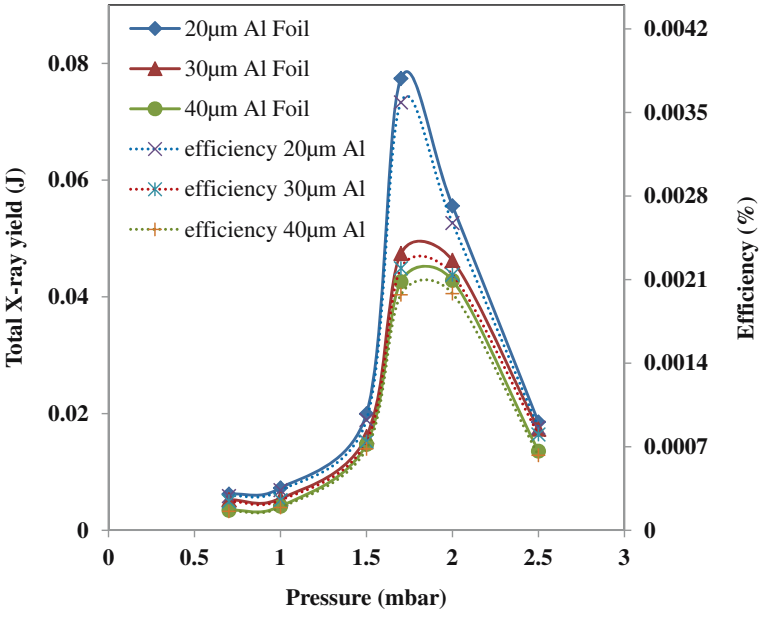

Figure 9. Variations of total X-ray yield in 4π-geometry and efficiency vs. argon gas pressure at a constant applied voltage of 12 kV.

ranging from 3 to 7 keV and pressures ranging from 1.0 to 2.5 mbar. The calculated electron temperatures from R at the given pressure range are shown in figure 10.

The ratio curves for all peaks between 1.5 and 2.0 mbar lie close to the absorption curve for Cu radiation. This result implied that the plasma was largely contaminated with Cu impurities related to the X-ray emission from Cu-K_α line. The X-rays were ascribed to the interactions of energetic electrons with the hollow Cu anode. In plasma focus, the energetic electron beams are dependent on the gas pressure [32]. The electron beam intensity increases up to a specific optimum pressure and decreases for pressures higher or lower than the optimum value.

The results further revealed that our plasma focus device was highly contaminated with Cu impurities. Therefore, the radiations primarily originated from the Cu impurities generated from the bombardment of energetic electrons with the hollow anode surface.

The maximum electron temperature was 7 keV, and the maximum total X-ray yields were 77 (20 and 100 μm Al foil), 47 (30 and 100 μm Al foil), and 42 mJ (40 and 100 μm Al foil) at the optimum 1.7 mbar argon gas pressure.

The PMT and HV signals at 1.7 mbar obtained by the interactions of the energetic electron beams are shown in figure 11.

PMT was used to determine the temporal behaviour of electron beams emission from the plasma focus. The strong electron beams were observed from 1.5 to 2.0 mbar. The radiation intensity was attributed to the strong bombardment of energetic electron beams on the target, which was adjusted at 45°.

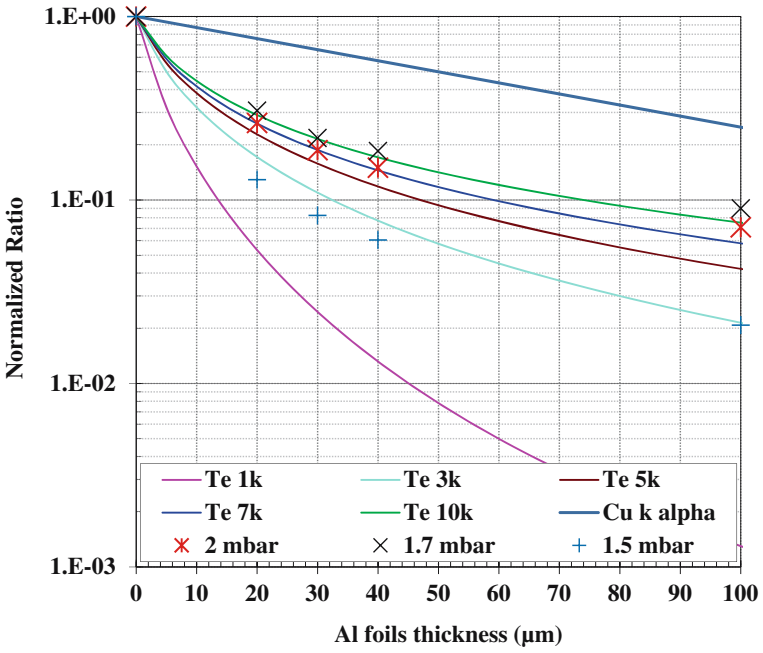

Figure 10. The calculated absorption curves of Al foils for X-rays from copper plasma at various temperatures and X-rays with argon gas pressures of 1.5, 1.7, and 2.0 mbar with the estimated electron temperatures 3, 7 and 6 keV, respectively.

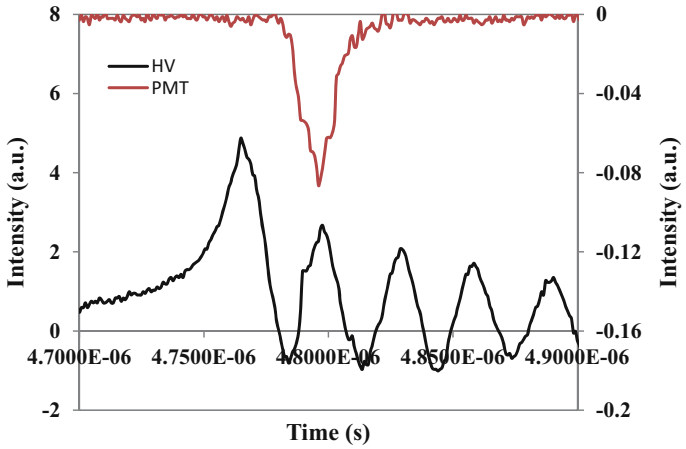

Figure 11. Typical signals of PMT with HV probe.

The average HXR intensity obtained by the energetic electron beam between 1.0 and 2.0 mbar is shown in figure 12. The HXR intensity increased in the aforementioned pressure because of the bombardment of the electron beams. The maximum average intensity was recorded by PMT at 1.7 mbar.

This result implied the importance of energetic electron beam emission from the plasma focus region in low-energy plasma focus devices. This beam emission was attributed to instabilities.

XR100CR X-ray spectrometer was used to trace the X-ray line spectrum. This equipment can be used in the analysis of X-ray energy distribution. In our experiment, the X-ray spectrometer was used at the side-on position 4 cm away from the lead target at 45°. The X-ray line spectrum exhibited energies of 8.07, 8.67, and 10.42 keV corresponding to Cu-$K_{\alpha 1}$, Cu-$K_{\beta 1}$, and Pb-$L_{\alpha 2}$ lines. Furthermore, the spectrum was obtained with

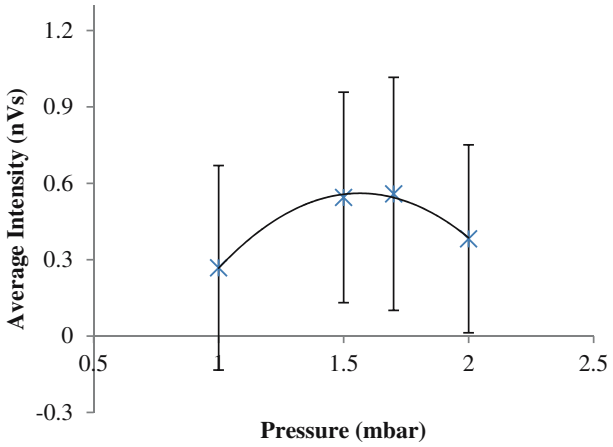

Figure 12. Variations of X-ray intensities with PMT vs. pressure (mbar).

the temporal evolution of X-ray pulses at a specific Al foil thickness and 1.7 mbar pressure. X-ray1 (23 μm aluminized Mylar +30 μm Al foil) and X-ray2 (23 μm aluminized Mylar+20 μm Al foil) with the typical HV probe and RC signals are shown in figure 13.

Spectrometric results supported the energetic electron beam emission from the focal region due to instabilities upon collision with the target material. The energetic electron

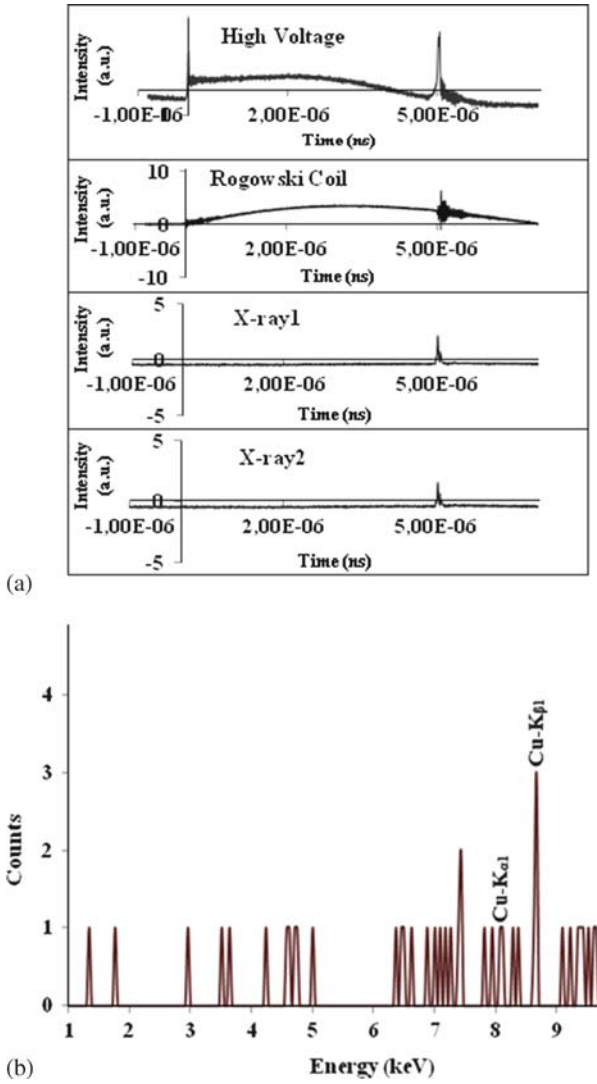

Figure 13. (**a**) Temporal evolution of X-ray pulses at a specific Al foil thickness for a pressure of 1.7 mbar, X-ray1 (23 μm aluminized Mylar + 30 μm Al foil), X-ray2 (23 μm aluminized Mylar + 20 μm Al foil) with the typical HV and RC signals. (**b**) X-ray spectrum: X-rays produced by the energetic electron beam target effect at an angle of 45° when the spectrometer is at side-on position.

Figure 14. Picture of the lead target after bombardment of energetic electron beam from the focus.

beam energy was high enough to Pb-$K_{\alpha 1}$ radiation in the X-ray line spectrum. However, it is impossible to detect this radiation by the present spectrometer because of constraints in its energy range.

High electron temperature of 7 keV was measured at 1.7 mbar because of the instabilities. The calculated electron temperature ranged from 3 to 7 keV at 1.5 and 2.0 mbar and a constant applied voltage of 12 kV. This result verified the maximum electron temperature and maximum total X-ray yield at 1.7 mbar using pairs of Al foils. Furthermore, X-ray yield, energetic electron beam energy, and electron temperature of the argon plasma were achieved at 1.5–2.0 mbar because of the strong bombardments of the electron beam. The result was essential in our plasma focus device which uses the hollow anode.

An image of the target is shown in figure 14, which reveals a considerable interaction of the energetic electron beam on the target.

4. Conclusions

A low-energy plasma focus device (2.2 kJ, 12 kV) was studied as an electron beam and an X-ray source. The maximum electron temperature of the plasma was 7 keV. Maximum total X-ray yields were 77, 47, and 42 mJ with corresponding efficiencies of 0.0035, 0.0021, and 0.0018% at the optimum argon pressure of 1.7 mbar and a constant applied voltage of 12 kV. The X-ray spectrum revealed Cu-$K_{\beta 1}$ and Pb-$L_{\alpha 2}$ lines at the 45° side-on position of the lead target at optimum pressure. Thus, the electron temperature, X-ray yield, and electron beam energy were obtained under argon plasma from 1.5 to 2.0 mbar. The results supported the important function of the energetic electron beam from the plasma focus with a hollow anode of new dimensions. The results will contribute to the analyses of electron beams emission in applied sciences and other related fields.

Acknowledgements

The authors acknowledge the technical support from Mr Jasbir Singh. This work was supported by the University of Malaya (Grant No. RG102-10AFR).

References

[1] J W Mather, *Phys. Fluids (Suppl.)* **7**, 5 (1960)
[2] Y Kato, I O Chiai, Y Watanabe and S J Murayama, *J. Vac. Sci. Technol. B* **6**, 195 (1988)
[3] Y Kato and S H Be, *Appl. Phys. Lett*. **48**, 686 (1986)
[4] P Lee, X Feng, G X Zhang, M H Liu and S Lee, *Plasma Sources Sci. Technol*. **6**, 343 (1997)
[5] F Castillo-Mejia, M M Milanese, R L Moroso, J O Pouzo and M A Santiago, *IEEE Trans. Plasma Sci.* **29**, 921 (2001)
[6] H Kelly, A Lepone, A Marquez, D Lamas and C Oviedo, *Plasma Sources Sci. Technol.* **5**, 704 (1996)
[7] V A Gribkov, A Srivastava, P L C Keat, V Kudryashov and S Lee, *IEEE Trans. Plasma Sci.* **30**, 1331 (2002)
[8] M Zakaullah, K Alamgir, M Shafiq, M Sharif and A Waheed, *IEEE Trans. Plasma Sci.* **30**, 2089 (2002)
[9] F N Beg, I Ross, A Lorenz, J F Worley, A E Dangor and M G Haines, *J. Appl. Phys.* **88**, 3225 (2000)
[10] R Lebert, W Neff and D Rothweiler, *J. X-ray Sci. Technol*. **6**, 107 (1996)
[11] K Hirano, T Yamamoto, S Takada, H Sone and K Shimoda, *Jpn J. Appl. Phys.* **27**, 89 (1988)
[12] M Zakaullah, K Alamgir, M Shafiq, S M Hassan, M Sharif and A Waheed, *Appl. Phys. Lett.* **78**, 877 (2001)
[13] S Lee and C S Wong, *Phys. Today* **59**, 31 (2006)
[14] F C Jahoda, E M Little, W E Quinn, G A Sawyer and T F Stratton, *Phys. Rev*. **119**, 843 (1960)
[15] M J Bernstein, *Phys. Fluids* **13**, 2858 (1970)
[16] S L Yap, C S Wong, P Choi, C Dumitrescu and S P Moo, *Jpn J. Appl. Phys*. **44**, 8125 (2005)
[17] K Ranjini, P Y Nabhiraj, S K Das, C Mallik and R K Bhandari, *Indian J. Pure Appl. Phys.* **45**, 965 (2007)
[18] Sh Al-Hawat, M Akel and C S Wong, *J. Fusion Energy* **30**, 503 (2011)
[19] S Hussain, S Ahmad, M Z Khan, M Zakaullah and A Waheed, *J. Fusion Energy* **22**, 195 (2003)
[20] M Zakaullah, K Alamgir, G Murtaza and A Waheed, *Plasma Sources Sci. Technol.* **9**, 592 (2000)
[21] H L L van Paassen, R H Vandre and R S White, *Phys. Fluids* **13**, 2606 (1970)
[22] W L Harries, J H Lee and D R McFarland, *Plasma Phys.* **20**, 95 (1978)
[23] J Pouzo, H Acuna, M Milanese and R Moroso, *Eur. Phys. J. D* **21**, 97 (2002)
[24] J R Smith, C M Luo, M J Rhee and R F Schneider, *Phys. Fluids* **28**, 2305 (1985)
[25] K Hirano, I Kaneko, K Shimoda and T Yamamoto, *Jpn J. Appl. Phys.* **29**, 1182 (1990)
[26] W Styger, G Gerdin, F Venneri and J Mandrekas, *Nucl. Fusion* **22**, 1161 (1982)
[27] S R Mohanty, H Bhuyan, N K Neog, R K Rout and E Hotta, *Jpn J. Appl. Phys*. **44**, 5199 (2005)
[28] G Modreanu, N B Mandache, A M Pointu, M Ganciu and I I Popescu, *J Phys. D: Appl. Phys.* **33**, 819 (2000)
[29] M Zakaullah, K Alamgir, M Shafiq, M Sharif, A Waheed and G Murtaza, *J. Fusion Energy* **19**, 143 (2000)
[30] M Z Khan, S L Yap and C S Wong, *Int. J. Phys. Sci.* **8**, 286 (2013)
[31] M Z Khan, S L Yap, M A Khan, A U Rehman and M Zakaullah, *J. Fusion Energy* **32**, 34 (2013)
[32] J R Smith, C M Luo, M J Rhee and R F Schneider, *Phys. Fluids* **28**, 2305 (1985)